SHIMURA, T. & HARADA, J. (1993). *J. Appl. Cryst.* **26**, 151–158.
STEPANOV, S. A. (1994). *Crystallogr. Rep.* **39**, 182–187.
STEPANOV, S. A. & KOHLER, R. (1994). *J. Appl. Phys.* **78**, 7809–7815.
VINEYARD, G. H. (1982). *Phys. Rev. B*, **26**, 4146–4159.
ZACHARIASEN, W. H. (1967). *Theory of X-ray Diffraction in Crystals*. New York: Dover.

Acta Cryst. (1995). A**51**, 931–936

Single-Crystal Data Collection with a Laue Diffractometer

BY J. LANGE AND H. BURZLAFF

Institut für Angewandte Physik, Lehrstuhl für Kristallographie der Universität Erlangen-Nürnberg, Bismarckstrasse 10, 91054 *Erlangen, Germany*

(*Received* 17 *June* 1994; *accepted* 20 *July* 1995)

Dedicated to Professor Dr M. M. Woolfson

Abstract

The Laue technique is suitable to study effects that depend on wavelength such as absorption, anomalous dispersion or secondary extinction. The accuracy of the measured integrated intensities for X-ray structure determination is comparable with measurements of conventionally collected data. The present paper describes and discusses the results of a single-crystal data collection with a Laue diffractometer. The results obtained from the Laue data are in very good agreement with the results from conventionally collected data.

Introduction

The availability of synchrotrons as white-radiation X-ray sources of high spectral brilliance is the reason for recent developments in Laue diffraction techniques for data collection, especially in the field of protein crystallography. Several two-dimensional detector systems are in use, such as films (*e.g.* Rabinovich & Lourie, 1987), image plates (*e.g.* Miyahara, Takahashi, Amemiya, Kamiya & Satow, 1986), multiwire proportional chambers (*e.g.* Baru *et al.*, 1978), the FAST system (Bartunik & Borchert, 1989) and others (*International Tables for Crystallography*, 1992).

Since it is the primary intention in this field to increase the speed of data collection, less attention is paid to the accuracy of a single measurement. Only one attempt (Sakamaki, Hosoya & Fukamachi, 1980) has been made to incorporate the Laue technique into an ordinary four-circle-diffractometer device. The present authors reported in a series of short communications on the hardware development of devices suitable for this purpose (Lange & Burzlaff, 1991*a*,*b*).

It is the intention of this paper to report first results on the basis of a medium-sized inorganic structure, to compare the data with a data set collected in the classical way and to discuss the results and the technique in comparison with the work of Sakamaki *et al.*

Measurement of integrated intensities

Single-crystal X-ray diffraction with white radiation differs from the monochromatic technique in the following ways:

1. Instead of one well defined Ewald sphere with radius $R = 1/\lambda$, a continuous distribution of Ewald spheres with $R_{\min} \leq R \leq R_{\max}$ is present resulting in a simultaneous diffraction process for a large number of reciprocal-lattice vectors $\mathbf{h}_i$. Each vector $\mathbf{h}_i$ selects its own Ewald sphere depending on its position in the reciprocal space.

For the simultaneous registration of the reflections, a two-dimensional detector is necessary that allows the angular localization of the diffracted beams. In addition, the wavelength distribution within the diffracted beam has to be known. Approximately 17% (Cruickshank, Helliwell & Moffat, 1987) of all diffracted beams contain a series of $n\lambda$ related to the scattering vectors $n\mathbf{h}$ of the reflection ($n = 1, 2, 3, \ldots$).

2. In contrast to the conventional monochromatic technique, a property of the crystal is utilized in another way. With the model for a real crystal composed of small mosaic blocks, the end point of the scattering vector **h** must be replaced by a small fragment of a spherical surface. Its shape is determined by the mosaic-block distribution of the crystal.

With monochromatic radiation, scan procedures must be applied to obtain the integrated intensity originating from all mosaic blocks. In the case of white-beam diffraction, all mosaic blocks are in scattering position simultaneously since a bundle of Ewald spheres (close to the 'main' Ewald sphere for the reflection corresponding to **h**) is present. No scan process is necessary for the measurement of the integrated intensity provided that the detector is suitable to collect the entire diffracted beam.

It is the basic idea of this paper to make use of the second point above concerning a single reflection **h**. In order to determine the wavelengths related to a

Laue reflection, the detector must be supplied with a multichannel analyser.

This technique is more flexible than the use of a conventional diffractometer since the experiment is not restricted to the wavelength of one characteristic line but a suitable wavelength λ can be selected within the range of the white radiation. These considerations lead to the construction of a Laue diffractometer as described by the authors (Lange & Burzlaff, 1992).

According to the previous considerations, two different measuring techniques are possible with the Laue diffractometer.

1. *Polychromatic technique* (*PMT*). The PMT is similar to the classical Laue technique and uses the entire white X-ray spectrum. The orientation of the single crystal is fixed and the film plate is replaced by the scintillation counter with multichannel analyser. The detector can be moved to a single reflection position in order to measure the integrated intensity and the wavelengths within the Laue reflection.

The PMT is used before an orientation matrix is available. In order to calculate an orientation matrix, a field of directions $(\Theta, \nu) \in ([\Theta_{\min}, \Theta_{\max}], [\nu_{\min}, \nu_{\max}])$ is scanned by the detector. Θ and ν are the detector axes. The reciprocal coordinates $\mathbf{h}_i = (h_x, h_y, h_z)_i$ of the detected reflections in $([\Theta_{\min}, \Theta_{\max}], [\nu_{\min}, \nu_{\max}])$ are calculated. From this, the orientation matrix is determined in the usual way.

2. *Quasimonochromatic technique* (*QMT*). After the determination of the orientation matrix by the PMT, the QMT can be applied to the refinement of the orientation matrix and to the data-collection process. In this case, the scattering vector $\mathbf{h}$ is moved to one diffraction position at a selected wavelength λ_q. All reflections can be treated in the same way concerning absorption and other effects depending on wavelength.

Laue diffractometer

A detailed description of the diffractometer is given by Lange & Burzlaff (1992). Here, some characteristic properties are summarized:

1. *Four-circle diffractometer* (Burzlaff, Lange & Rothammel, 1987). Two crystal axes (ω, δ) with inclination angle of 30°, two perpendicular detector axes (Θ, ν), Θ and ω are coaxial. Crystal–tube distance: 400 mm.

2. *Tube*. Tungsten anode, 50 kV, 40 mÅ. Unfiltered spectrum without characteristic lines within the interval [0.248, 1.02Å]. Wavelength of QMT: $\lambda_q = 0.46$ Å $\widehat{=}$ 26.95 keV.

3. *Detector device*. Photomultiplier with NaI(Tl) scintillation crystal. Energy resolution: 46% at 5.9 keV. Multichannel analyser (MCA) with 1024 channels (Lange & Burzlaff, 1991*a*).

In order to achieve high accuracy, important properties and parameters of the detector system and the X-ray source were investigated and used for data correction:

1. *Calibration*. To a first approximation, the channel number of the MCA is proportional to the energy. This relation is not sufficient for high-accuracy measurements since deviations from the linearity are observed (up to 15%). The reason for these deviations is the absorption behaviour of the NaI scintillation crystal depending on the wavelength (*e.g.* Aitken, Beron, Yenicay & Zullinger, 1967).

2. *Temperature stability of the detector system*. The calibration depends also on the temperature of the detector. An investigation led to a value of 0.2%/1 K for the change of the detector-signal amplitudes.

3. *Energy resolution*. To a first approximation, the energy resolution of the detector is $\Delta E/E \propto 1/E^{1/2}$. A detailed investigation led to the result that there are deviations up to 10% from this relation.

4. *X-ray spectrum*. The maximum counting rate within the white spectrum is at $\lambda_m = 0.49$ Å $\widehat{=}$ 25.30 keV. λ_m depends on the tube voltage, thickness of the scintillation crystal *etc.* and is close to λ_q.

With the QMT at λ_q and a tube voltage of 50 kV, the second order of $\mathbf{h}$ cannot appear in the energy spectrum of the Laue reflection and the main peak at λ_q is not modified by escape peaks (see *e.g.* Kaelble, 1967; *International Tables for X-ray Crystallography*, 1962).

5. *Polarization of the white X-ray spectrum*. In order to determine the degree of polarization, some reflections were investigated applying the QMT at λ_q. Some scattering vectors $\mathbf{h}$ were moved around the δ axis step by step. Each δ position δ_i leads to a pair of detector angles (ν_i, Θ_i). If the beam were partially polarized, a systematic change of the reflection intensity should be observed. Since no polarization could be observed, the polarization factor for unpolarized radiation was used for the collected data.

High-accuracy Laue data may be expected when the properties of the detector and the X-ray spectrum are taken into account and when a wavelength of $\lambda_q = 0.46$ Å is selected. According to Kramers's (1923) theory, the efficiency of the production of X-rays is

$$\eta = \frac{\text{X-ray energy}}{\text{cathode ray energy}} = 9.2 \times 10^{-10} ZU, \quad (1)$$

with U in V. The efficiency of the tungsten tube ($Z = 74$) at $U = 50$ kV is 0.34%. With Pt or Au tubes ($Z = 78, 79$), the efficiency cannot be increased remarkably; other tubes such as Ag, Mo or Cu ($Z = 42, 47, 29$) lead to much lower efficiencies.

Data collection

The test crystal for the data collection was a Zn-D'Ansite single crystal [spherical with diameter 0.38 (3) mm]. This compound is a salt with the composition $(ZnSO_4)$-$3(NaCl)9(Na_2SO_4)$ and $Z = 4$. Burzlaff & Grube (1980) reported investigations of twinned Zn-D'Ansite single crystals. According to their paper, the space group is $I\bar{4}3d$. The lattice parameter is $a = 15.9132(5)$ Å, $\mu(0.46\text{ Å}) = 4.5\text{ cm}^{-1}$ and $F(000) = 3092$. This crystal was chosen because an accurate data set (Burzlaff & Grube, 1980) was available, measured with Mo $K\alpha$ radiation and a single-crystal diffractometer (Hilger & Watts Y290). The determination of the metric by the different Laue techniques was performed in two steps:

1. *Determination of the metric by the PMT.* From 15 Laue reflections related to 24 scattering vectors, a preliminary orientation matrix was calculated with lattice parameters $a = 15.7(2)$ Å, $\alpha = 90(1)°$.

The orientation matrix was calculated in the usual way (*e.g.* Gomm, 1993) from the coordinates $(h_x, h_y, h_z)_i$ of the scattering vectors $\mathbf{h}_i$ $(i = 1, 2, \ldots, 24)$. The coordinates of each scattering vector $\mathbf{h}_i$ depend on the angles ω_i, δ_i, Θ_i, ν_i and the energy E_i.

2. *QMT refinement.* The orientation matrix determined by the polychromatic procedure is accurate enough to start a refinement at 0.46 Å. The refinement with the 123 reflection and its symmetrical equivalents leads to $a = 15.913(9)$ Å, $\alpha = 90.01(2)°$.

All reflections were measured within $0 \leq 2\Theta \leq 43°$ for $-26 \leq (h, k) \leq 26$, $-26 \leq l \leq 1$ at 300 K; standard reflections were 510 and 910, measured after each 250 reflections; measurement time for each reflection was 55 s. The detector aperture was 3 mm in diameter. 13 505 Laue reflections were measured including systematically absent reflections due to the $d_{[1\bar{1}0]}$ glide plane; 807 unique reflections were obtained after merging; 92 reflections with $|F| \leq 3\sigma$ were removed from the data set, 33 systematically absent reflections due to the $d_{[1\bar{1}0]}$ glide plane were also removed.*

*A list of structure factors has been deposited with the IUCr (Reference: SH0055). Copies may be obtained through The Managing Editor, International Union of Crystallography, 5 Abbey Square, Chester CH1 2HU, England.

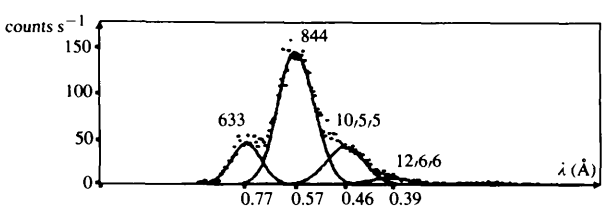

Fig. 1. Laue reflection with several orders: 633 at 0.77 Å, 844 at 0.57 Å, 10,5,5 at 0.46 Å and 12,6,6 at 0.39 Å. Crystal: Zn-D'Ansite, space group $I\bar{4}3d$, $a = 15.913$ Å.

Table 1. *Fractional coordinates*

Values given in the second line for each atom result from monochromatic data.

	x	y	z
Na/Zn	0.3293 (1)	0.3293 (1)	0.3293 (1)
	0.32956 (7)	0.32956 (7)	0.32956 (7)
Cl	0.25000	0.37500	0.00000
	0.25000	0.37500	0.00000
S(1)	0.25000	0.2683 (1)	0.50000
	0.25000	0.26827 (6)	0.50000
S(2)	0.46086 (9)	0.46086 (9)	0.46086 (9)
	0.46069 (5)	0.46069 (5)	0.46069 (5)
Na(1)	0.3748 (1)	0.3488 (1)	0.1180 (1)
	0.37487 (9)	0.34864 (8)	0.11778 (9)
Na(2)	0.5177 (7)	0.246 (1)	0.4570 (2)
	0.5178 (2)	0.2454 (5)	0.4567 (2)
O(1)	0.0863 (2)	0.4761 (2)	0.4637 (2)
	0.0878 (2)	0.4747 (2)	0.4638 (2)
O(2)	0.2320 (2)	0.0344 (2)	0.4263 (2)
	0.2319 (2)	0.0338 (1)	0.4260 (2)
O(3)	0.0180 (2)	0.3231 (2)	0.0725 (2)
	0.0180 (2)	0.3229 (2)	0.0724 (2)
O(4)	0.4091 (3)	0.4091 (3)	0.4091 (3)
	0.4086 (3)	0.4086 (3)	0.4086 (3)

A full-matrix least-squares program fits a sum of Gaussian functions to the energy peaks of the measured Laue-reflection spectrum

$$S(E) = \sum_{i=1}^{j} G_i(E) = \sum_{i=1}^{j} A_i \exp[(E - E_i)^2/B_i^2]. \quad (2)$$

A_i is the amplitude, E_i the center of the peaks, B_i determines the width of the peaks and j is the number of peaks in the spectrum. An example with several orders within a Laue reflection is shown in Fig. 1. This example illustrates the counting rate per channel and the result of the fitting process.

The standard deviation σ of a reflection was determined by $\sigma(|F|^2) = (\sigma_I^2 + \sigma_A^2 + \sigma_B^2 + \sigma_U^2)^{1/2}$. The standard deviation resulting from the statistical error is $\sigma_I = N^{1/2}$ with

$$N = \int_{-\infty}^{+\infty} G_i(E)\,dE = \pi^{1/2} A_i B_i. \quad (3)$$

σ_A and σ_B are the estimated standard deviations of A_i and B_i calculated from the general equation of the least-squares procedure (*e.g. International Tables for X-ray Crystallography*, 1959). The standard deviation of the background N_U is $\sigma_U = N_U^{1/2}$.

The least-squares procedure does not always converge if $j > 3$. In this case, the calculated energies E_i and peak widths B_i are not refined. The least-squares start values for the parameters A_i are calculated from the measured spectra by a recursive algorithm that considers the neighbouring peaks $i + 1$ and $i - 1$. In this way, a stable convergence of the least-squares procedure is guaranteed. This special procedure allows the separation of up to six overlapping orders $n\mathbf{h}$ unambiguously within

the energy spectrum, in spite of the poor resolution of the detector.

The background-correction program used a background function $B(\theta, \lambda)$ (θ = diffraction angle), which was evaluated separately in a first attempt. The results were not satisfactory since the 33 systematically absent reflections of the glide plane did not vanish in the statistical average after the background correction with $B(\theta, \lambda)$. An additional background correction led to improved results applying the following procedure:

With the significant net intensities of the 33 systematically absent reflections obtained with the background correction $B(\theta, \lambda)$, a new background data field $N_U(\theta_i)$ with $1 \leq i \leq 33$ was generated. The angles θ_i are the diffraction angles (at 0.46 Å) of the systematically absent reflections and the values of N_U are the incompletely corrected integrated intensities of the systematically absent reflections. Values of $N_U(\theta)$ with $\theta_i < \theta < \theta_{i+1}$ were interpolated. All reflections were additionally corrected with this background function $N_U(\theta)$ by subtraction.

Results

The structure was refined using 682 reflections by full-matrix least squares based on $|F|$. Anisotropic displacement parameters were used for all atoms. The final R values were $R = 0.071$ and $R_w = 0.021$ (R values resulting from the monochromatic data are $R = 0.036$, $R_w = 0.036$).

According to Burzlaff & Grube (1980), the Zn^{2+} and $Na(1)^+$ ions are statistically distributed in the position 16(*c*) *xxx* (25% Zn^{2+} and 75% Na^+). This distribution leads to an occupation factor for $Na(1)^+$ of $f_{occ} = 1.45$. The values obtained from the monochromatic data and from the Laue data were $f_{occ} = 1.42(1)$ and $f_{occ} = 1.455(9)$, respectively. $f_{occ} = 1.455(9)$ is closer to the calculated value.

In addition, the $Na(2)^+$ ion does not occupy exactly the twofold axis; thus, it was set to a general position and treated as a split atom with $f_{occ} = 0.5$. The least-squares calculation using the monochromatic data set led to $f_{occ} = 0.459(6)$ while the use of the Laue data set resulted in $f_{occ} = 0.493(3)$, showing again better agreement with the calculated value.

Table 1 shows the fractional coordinates and Table 2 the displacement factors resulting from full-matrix least-squares refinement of both data sets. Comparison shows that no important deviations appear. Nearly all fractional coordinates agree within two standard deviations and the displacement coefficients agree within five standard deviations. Exceptions are the parameters x and y for O(1), which agree within four standard deviations, and U_{11}, U_{22} and U_{33} for S(2), which agree within seven standard deviations.

The extinction correction method of Larson (1970) leads to a parameter of 39 649 (σ = 3635) for the monochromatic and 13 108 (σ = 1271) for the Laue data set. Thus, the Laue technique is suitable to reduce the amount of extinction. The R values obtained by least squares without secondary extinction correction were $R = 0.074$ and $R_w = 0.024$ for the Laue data and $R = 0.043$ and $R_w = 0.043$ for the monochromatic data.

Table 3 shows some selected structure-factor moduli from the monochromatic and Laue data sets. The calculated values F_{cal} represent the structure-factor moduli without secondary-extinction correction from the least-squares procedure. In addition, the percentage deviation for the extinction effect is tabulated.

Discussion

It could be shown that surprisingly good crystallographic information can be obtained with the Laue technique in spite of the use of an ordinary scintillation detector. Similar measurements were performed by Sakamaki, Hosoya & Fukamachi (1980). They used a heavy and expensive solid-state detector cooled with liquid nitrogen. These authors describe several examples of data collections. They obtained a final R value of 2.12% at $E_2 = 25$ keV [$E_2 \simeq (hc)/\lambda_q$]. The overall quality of their example (LiF crystal sample) is comparable with the data quality of the present work ($R_w = 2.4$). It is not clear from the paper of Sakamaki *et al.* what kind of R value (weighted or unweighted) they mean.

Sakamaki *et al.* measured about four symmetrically equivalent reflections for each structure factor. The measurement time of each reflection was about 8.5 min, resulting in an effective measurement time t_1 for each structure-factor value of about $4 \times 8.5 = 34$ min on average.

In the present work, about 17 symetrically equivalent reflections were measured on average for each structure factor. This leads to a total measurement time of 17×55 s = 15.6 min. Furthermore, Sakamaki *et al.* used an X-ray tube with a Cu target at 40 kV and 20 mA. By application of (1) (tungsten: $Z = 74$, $U = 50$ kV, $I = 40$ mA; copper: $Z = 29$, $U = 40$ kV, $I = 20$ mA), the ratio of the efficiency factors η_W/η_{Cu} is about 6.4. The effective measurement time with a Cu tube would therefore have been $t_2 = 6.4 \times 15.6$ min = 100 min.

Comparing t_1 with t_2 gives a factor of only 3 in spite of the fact that the solid-state detector has a much better energy resolution. In general, the signal-to-noise ratio and data quality can be improved by using a detector with better energy resolution since the background correction can be performed much more reliably. The improvements of the present work are probably because additional corrections described earlier were applied to the Laue data.

On the other hand, the large difference between R and R_w shows that the improvements obtained by the additional corrections are limited. The signal-to-noise

Table 2. *Anisotropic displacement coefficients* U_{ij}

Values given in the second line for each atom result from monochromatic data.

	U_{11}	U_{22}	U_{33}	U_{23}	U_{13}	U_{12}
Na/Zn	0.0291 (9)	0.0291 (9)	0.0291 (9)	0.0085 (8)	0.0085 (8)	0.0085 (8)
	0.0334 (6)	0.0334 (6)	0.0334 (6)	0.0054 (5)	0.0054 (5)	0.0054 (5)
Cl	0.0173 (8)	0.012 (1)	0.0173 (8)	0.0000	0.0000	0.0000
	0.0224 (4)	0.0189 (5)	0.0224 (4)	0.0000	0.0000	0.0000
S (1)	0.022 (1)	0.0093 (9)	0.0124 (9)	0.0000	−0.0022 (9)	0.0000
	0.0266 (5)	0.0144 (3)	0.0169 (4)	0.0000	−0.0027 (4)	0.0000
S (2)	0.0132 (5)	0.0132 (5)	0.0132 (5)	0.0017 (6)	0.0017 (6)	0.0017 (6)
	0.0181 (2)	0.0181 (2)	0.0181 (2)	0.0012 (2)	0.0012 (2)	0.0012 (2)
Na (1)	0.022 (1)	0.028 (1)	0.021 (1)	−0.0021 (9)	−0.003 (1)	0.006 (1)
	0.0285 (6)	0.0300 (6)	0.0250 (6)	−0.0029 (5)	−0.0043 (6)	0.0036 (5)
Na (2)	0.052 (9)	0.029 (4)	0.011 (2)	−0.004 (4)	−0.003 (3)	−0.005 (7)
	0.047 (3)	0.036 (2)	0.016 (1)	0.000 (2)	−0.002 (1)	−0.005 (3)
O (1)	0.086 (3)	0.050 (3)	0.024 (2)	−0.007 (2)	0.033 (3)	−0.031 (3)
	0.078 (2)	0.056 (2)	0.039 (2)	−0.012 (1)	0.031 (2)	−0.028 (2)
O (2)	0.029 (2)	0.016 (2)	0.029 (2)	0.006 (2)	0.002 (2)	0.000 (2)
	0.033 (1)	0.026 (1)	0.032 (1)	0.0070 (9)	−0.001 (1)	−0.0000 (9)
O (3)	0.031 (3)	0.034 (2)	0.032 (2)	−0.026 (2)	0.001 (2)	−0.010 (2)
	0.043 (2)	0.043 (1)	0.037 (1)	−0.024 (1)	−0.001 (1)	−0.009 (1)
O (4)	0.093 (3)	0.093 (3)	0.093 (3)	−0.032 (3)	−0.032 (3)	−0.032 (3)
	0.109 (4)	0.109 (4)	0.109 (4)	−0.040 (3)	−0.040 (3)	−0.040 (3)

Table 3. *Observed and calculated structure-factor moduli*

	Laue data				Monochromatic data			
(*hkl*)	F_{obs}	ΔF_{obs}	F_{cal}	dev. (%)	F_{obs}	ΔF_{obs}	F_{cal}	dev. (%)
(400)	360.5	1.2	362.7	0.6	317.4	1.4	339.6	7
(800)	321.0	1.3	312.5	−2.7	297.1	1.2	310.4	4.5
(620)	311.0	0.7	311.7	0.2	288.8	1.0	305.3	5.7
(440)	645.5	2.3	718.0	11.2	486.9	1.8	692.7	42.3
(880)	336.7	1.7	341.5	1.4	307.2	1.0	320.5	4.3
(611)	261.3	0.6	261.1	−0.1	245.4	0.9	256.3	4.4
(332)	375.1	0.8	379.6	1.2	327.8	1.2	391.1	19.3
(552)	259.3	0.8	258.3	−0.4	243.2	0.8	249.9	2.8
(444)	346.6	1.1	343.5	−0.9	313.9	1.6	336.7	7.3
(664)	225.5	0.7	226.2	0.3	214.2	0.8	219.1	2.3
(655)	335.0	0.8	329.5	−1.6	309.1	1.1	323.9	4.8
(888)	275.2	1.7	270.5	−1.7	247.6	2.0	251.8	1.7

ratio for weak reflections can be considerably improved only by using a detector with a better energy resolution. A further improvement of the signal-to-noise ratio can be obtained by using varying detector apertures fitted to the optimal spot size of the Laue reflection. The spot size depends on the mosaic distribution, beam divergence *etc.* (*e.g.* Helliwell, 1992).

In addition, the data quality can be improved by using high-intensity X-ray sources. The use of the tungsten tube (2 kW) increases the efficiency η_W/η_{Cu} to 6.4 compared with the copper tube (0.8 kW) of Sakamaki *et al.*

In general, the intensity of a characteristic line is about two orders of magnitude stronger than the intensity per wavelength interval within the *Bremsstrahlung* spectrum. This does not mean that all integrated intensities of a Laue data set are two orders of magnitude weaker than that of a conventionally measured data set. With monochromatic radiation, the characteristic line selects an interval of the mosaic spread. Without a change of any other parameters, an increasing mosaic spread and beam divergence leads to an increasing width of the Bragg reflection. The consequence is an increase in the integrated measurement time without an additional gain of net intensity.

In contrast to the monochromatic technique, the mosaic spread selects a wavelength interval $\Delta\lambda$ when using white radiation. $\Delta\lambda$ increases when the mosaic spread and the beam divergence increases, with the consequence that a greater fraction of the incoming radiation of the primary beam is actually diffracted by the crystal sample. Thus, the measurement time can be reduced to obtain the same integrated intensity. A detailed discussion of the mosaic spread and beam divergence in the Laue technique can be found in Lange (1995).

Furthermore, the ratio of the Lorentz factors for monochromatic (with equatorial geometry) and white-beam diffraction is $\cot\theta$. This leads to an additional reduction of the measurement time, especially at low θ angles. This effect is discussed briefly in the paper of Sakamaki *et al.*

References

AITKEN, D. W., BERON, B. L., YENICAY, G. & ZULLINGER, H. R. (1967). IEEE *Trans. Nucl. Sci.* **NS-14**, 468.

BARTUNIK, H. D. & BORCHERT, T. (1989). *Acta Cryst.* A**45**, 718–726.

BARU, S. E., PROVIZ, G. I., SAVINOV, G. A., SIDOROV, V. A., KHABAKHSHEV, A. G., SHUVALOV, B. N. & YAKOVLEV, V. A. (1978). *Nucl. Instrum. Methods*, **152**, 209–212.

BURZLAFF, H. & GRUBE, H.-H. (1980). *Z. Kristallogr.* **152**, 83–93.

BURZLAFF, H., LANGE, J. & ROTHAMMEL, W. (1987). *Acta Cryst.* A**43**, C267.

CRUICKSHANK, D. W. J., HELLIWELL, J. R. & MOFFAT, K. (1987). *Acta Cryst.* A**43**, 656–674.

GOMM, M. (1993). *Crystallographic Computing* 6, pp. 6–9. IUCr/Oxford Univ. Press.

HELLIWELL, J. R. (1992). *Macromolecular Crystallography with Synchrotron Radiation*, pp. 297–298. Cambridge Univ. Press.

International Tables for Crystallography (1992). Vol. C, edited by A. J. C. WILSON, pp. 538–555. Dordrecht/Boston/London: Kluwer Academic Publishers.

International Tables for X-ray Crystallography (1959). Vol. II, edited by J. S KASPER & K. LONSDALE, p. 330, equation (6). Birmingham: Kynoch Press. (Present distributor Kluwer Academic Publishers, Dordrecht.)

International Tables for X-ray Crystallography (1962). Vol. III, edited by C. H. MACGILLAVRY, G. D. RIECK & K. LONSDALE, pp. 152, 153. Birmingham: Kynoch Press. (Present distributor Kluwer Academic Publishers, Dordrecht.)

KAELBLE, E. F. (1967). *Handbook of X-rays*, pp. 3-1, 3-2, 3-27. New York: McGraw-Hill.

KRAMERS, H. A. (1923). *Philos. Mag.* **46**, 836–871.

LANGE, J. (1995). *Acta Cryst.* A**51**, 559–565.

LANGE, J. & BURZLAFF, H. (1991*a*). *J. Appl. Cryst.* **24**, 190–193.

LANGE, J. & BURZLAFF, H. (1991*b*). *J. Appl. Cryst.* **24**, 1060–1062.

LANGE, J. & BURZLAFF, H. (1992). *J. Appl. Cryst.* **25**, 440–443.

LARSON, A. C. (1970). *Crystallographic Computing*, p. 292, equation (22). Copenhagen: Munksgaard.

MIYAHARA, J., TAKAHASHI, K., AMEMIYA, Y., KAMIYA, N. & SATOW, Y. (1986). *Nucl. Instrum. Methods*, A**246**, 572–578.

RABINOVICH, D. & LOURIE, B. (1987). *Acta Cryst.* A**43**, 774–780.

SAKAMAKI, T., HOSOYA, S. & FUKAMACHI, T. (1980). *J. Appl. Cryst.* **13**, 433–437.

Acta Cryst. (1995). A**51**, 936–942

A New Quasiperiodic Tiling with Dodecagonal Symmetry

BY YASUNARI WATANABE AND TAKASHI SOMA

The Institute of Physical and Chemical Research, Wako-shi, Saitama 351-01 *Japan*

AND MASAHISA ITO

Department of Material Science, Faculty of Science, Himeji Institute of Technology, Kamigori, Ako-gun, Hyogo 678-12 *Japan*

(*Received* 7 *July* 1994; *accepted* 4 *July* 1995)

Abstract

A new quasiperiodic (QP) pattern with dodecagonal symmetry defined by a self-similar inflation/deflation rule is presented. The pattern consists of three kinds of base tiles, thin rhombus, regular triangle and square, and their self-similar inflation/deflation rule is shown to be derived from a regular zonogon with 12-fold symmetry. The self-similar transformation matrix for this pattern is derived and the quasiperiodicity is discussed.

1. Introduction

The properties of quasiperiodic tilings with dodecagonal symmetry have been discussed by several authors. The studies of quasiperiodic tilings with pentagonal and decagonal symmetry began with the discovery of Al–Mn (icosahedral phase) (Schechtman, Blech, Gratias & Cahn, 1984) and Al–Fe (decagonal phase) quasicrystals (Fung *et al.*, 1986). The structure of crystalline states with dodecagonal symmetry in the Ni–Cr amorphous phase (Ishimasa, Nissen & Fukano, 1985) gives clues to studies of quasicrystal modeling. A dodecagonal quasiperiodic tiling (DQPT) was first presented by the grid method and self-similar inflation (Stampfli, 1986), which contains regular triangles, squares and rhombi. Another approach for DQPT was proposed using a projection method (Yang & Wei, 1987). The projection and grid methods have been extended and generalized with 3-, 4-, 5-, 6-, 8- and 12-fold symmetry (Whittaker & Whittaker 1988; Socolar, 1989) and algebraic studies of dodecagonal tiling have been carried out in detail (Niizeki & Mitani, 1987). Recently, octagonal, decagonal and dodecagonal tilings have been summarized in relation to Amman bar grids (Lück, 1993). In this paper, a new DQPT is presented, which is characterized by a matching self-similar inflation/deflation rule in building self-similarity. The quasiperiodicity is verified by the fact that the ratios of numbers of constituent base tiles (regular triangle, square and rhombus) converge to an irrational number when the infinite iteration of the inflation is operated on each tile.